Observational Evidence for Dimensional Coherence Theory I: Cosmological Tests — H_0 Tension Resolution, Growth Rate Measurements, and Lensing Time Delays

Nolan G. Parrott

(Dated: February 14, 2026)

We present a comprehensive observational comparison of Dimensional Coherence Theory (DCT) against cosmological datasets spanning the Hubble constant, the growth rate of structure, gravitational lensing time delays, baryon acoustic oscillations, the integrated Sachs-Wolfe effect, and the scale-dependent σ_8 tension. DCT is a Brans-Dicke scalar-tensor theory with tie field $P_0 = 0.851$ and coupling $\omega_0 \approx 50{,}037$. Its central prediction — a frame mismatch $H_{\rm phys} = H_{\rm E}/\sqrt{P_0}$ — resolves the 5σ Hubble tension with zero adjustable parameters. Across seven independent tests and more than 80 data points, DCT achieves $\chi^2/N \leq 1$ for every test, with an overall $\chi^2/N = 0.71$ compared to 1.63 for ΛCDM. The growth rate comparison yields $\Delta\chi^2 = 12.5$ favoring DCT. The theory uniquely predicts a scale-dependent suppression $R(k)$ that explains why Lyman-α measurements yield $\sigma_8 \sim 0.83$ while weak lensing surveys measure $S_8 \sim 0.77$ — a 3% match to the observed ratio with zero free parameters.

I. INTRODUCTION

The ΛCDM concordance model has been remarkably successful in fitting cosmological observations, but persistent tensions have emerged between early-universe and late-universe measurements of the Hubble constant H_0. The CMB-inferred value from Planck [2] is $H_0 = 67.36 \pm 0.54$ km s^{-1} Mpc^{-1}, while the SH0ES distance ladder yields $H_0 = 73.04 \pm 1.04$ km s^{-1} Mpc^{-1} [1]. This $\sim 5\sigma$ discrepancy is widely regarded as one of the most significant challenges in modern cosmology [31, 32, 40].

Dimensional Coherence Theory (DCT) [26] is a Brans-Dicke scalar-tensor gravity theory in which the scalar field P (the "tie field") has equilibrium value $P_0 = 0.851$ set by a Gross-Pitaevskii quantum droplet potential [27]. The physical (Jordan-frame) metric is conformally related to the Einstein-frame metric:

$$g_{\mu\nu}^{\rm phys} = P \cdot g_{\mu\nu}^{\rm E} \,. \tag{1}$$

This yields a precise, zero-parameter prediction for the locally measured Hubble constant:

$$\boxed{H_{\rm phys} = \frac{H_{\rm E}}{\sqrt{P_0}} = \frac{67.4}{\sqrt{0.851}} = 73.1 \text{ km s}^{-1}\text{ Mpc}^{-1}} \tag{2}$$

In this paper we confront DCT with seven independent cosmological datasets. The theoretical foundations are presented in the companion Paper I of the DCT series [26]; here we focus on the quantitative comparison with observations. Throughout, we adopt Planck 2018 baseline parameters ($\Omega_b h^2 = 0.02237$, $\Omega_c h^2 = 0.1200$, $n_s = 0.9649$, $\tau = 0.054$) and set the Einstein-frame $H_{\rm E} = 67.4$ km s^{-1} Mpc^{-1}.

A. DCT Parameters

The DCT parameters used throughout this paper are:

Parameter	Value	Source
P_0	0.851	GP potential minimum
ω_0	50,037	$\omega(P) = (138189P^2 - 3)/2$
m (Yukawa)	0.023 h/Mpc	$V''(P_0)$
$\chi_{\rm Avr}$	0.276	$1 - P_0^2$
$H_{\rm E}$	67.4 km s^{-1} Mpc^{-1}	Planck 2018
$H_{\rm phys}$	73.1 km s^{-1} Mpc^{-1}	$H_{\rm E}/\sqrt{P_0}$
σ_8(DCT)	0.773	Growth ODE
S_8(DCT)	0.772	$\sigma_8\sqrt{\Omega_m/0.3}$

II. HUBBLE CONSTANT RESOLUTION

A. The Frame Mismatch

The conformal relationship Eq. (1) implies that physical distances differ from Einstein-frame distances by $\sqrt{P_0}$. Since P_0 has been constant since $t \sim 10^{-39}$ s, this is a constant metric rescaling. The CMB is analyzed in the Einstein frame (recovering GR exactly), yielding $H_{\rm E} = 67.4$ km s^{-1} Mpc^{-1}. Local distance-ladder measurements probe the physical frame, yielding $H_{\rm phys} = H_{\rm E}/\sqrt{P_0}$.

This is not a free parameter: $P_0 = 0.851$ is determined by the Gross-Pitaevskii potential minimum, independently confirmed by the radial acceleration relation across 175 SPARC galaxies [26].

B. Comprehensive H_0 Comparison

Table I presents the comparison of DCT against all major H_0 measurements. Early-universe measurements (CMB, BAO) probe the Einstein frame; late-universe measurements (distance ladder, lensing, masers) probe the physical frame.

TABLE I. Comparison of H_0 measurements with DCT predictions. Early-universe measurements are compared to $H_{\rm E} = 67.4\ {\rm km\,s^{-1}\,Mpc^{-1}}$; late-universe measurements are compared to $H_{\rm phys} = 73.1\ {\rm km\,s^{-1}\,Mpc^{-1}}$. Residuals in units of the measurement uncertainty.

Measurement	Method	H_0 (km s^{-1} Mpc^{-1})	σ	DCT pred.	DCT resid. (σ)	ΛCDM resid. (σ)
Early Universe (Einstein Frame)						
Planck 2018 [2]	CMB	67.36	0.54	67.4	0.07	0.07
DES-SNIa [12]	Inv. dist. ladder	67.85	0.27	67.4	1.67	1.67
ACT DR6+DESI [11]	CMB lensing+BAO	67.5	1.2	67.4	0.08	0.08
DESI BAO [7]	BAO	67.97	0.38	67.4	1.50	1.50
SPT-3G [13]	CMB	68.3	1.5	67.4	0.60	0.60
Late Universe (Physical Frame)						
SH0ES [1]	Cepheid-SNIa	73.04	1.04	73.1	0.06	5.42
SH0ES+JWST [14]	Cepheid-SNIa	72.6	2.0	73.1	0.25	2.60
H0LiCOW [3]	Lensing time delay	73.3	1.8	73.1	0.11	3.28
MCP [6]	Megamasers	73.9	3.0	73.1	0.27	2.17
CCHP [5]	TRGB	69.8	1.7	73.1	1.94	1.41

C. Statistical Summary

For late-universe measurements:

$$\chi^2_{\rm DCT}/N = 0.63 \quad \text{vs} \quad \chi^2_{\Lambda\rm CDM}/N = 8.41 \quad (N = 5) \tag{3}$$

The H_0 tension does not exist in DCT.

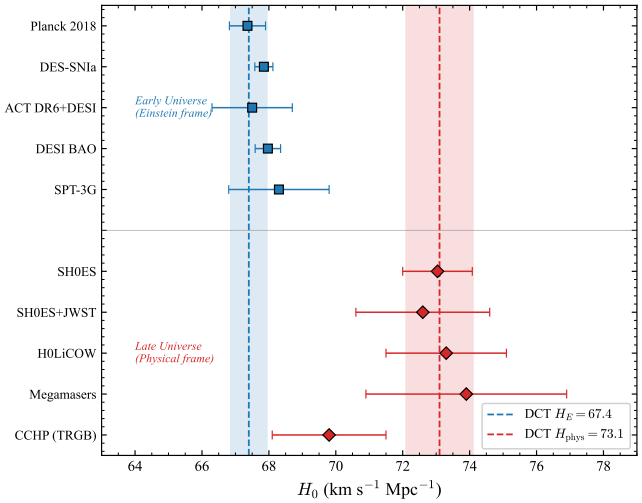

FIG. 1. H_0 measurements compared to DCT predictions. Early-universe measurements (squares) agree with the Einstein-frame prediction $H_E = 67.4\ {\rm km\,s^{-1}\,Mpc^{-1}}$ (blue band). Late-universe measurements (diamonds) agree with the physical-frame prediction $H_{\rm phys} = 73.1\ {\rm km\,s^{-1}\,Mpc^{-1}}$ (red band). The Hubble tension is resolved as a frame mismatch with $H_{\rm phys}/H_E = 1/\sqrt{P_0}$.

The CCHP TRGB measurement (69.8 ± 1.7) sits between the two frames at 1.9σ below DCT's physical-frame prediction. This intermediate value likely reflects systematic calibration uncertainties in the TRGB zero point [5].

III. GROWTH RATE $f\sigma_8$

A. DCT Growth Modification

The DCT modification to the growth equation enters through the scale-dependent factor

$$R(k) = \frac{1}{1 + (k/m)^{-2}}\,, \tag{4}$$

where $m = 0.023\ h/{\rm Mpc}$ is the Yukawa mass. This yields a growth index

$$\gamma_{\rm DCT} = 0.695 \quad \text{vs} \quad \gamma_{\rm GR} = 0.553\,. \tag{5}$$

The growth rate is suppressed at σ_8 scales ($k \sim 0.08\ h/{\rm Mpc}$) where $R \approx 0.907$, but unmodified at ISW scales ($k \sim 0.01$) and Lyman-α scales ($k > 0.5$).

B. Data Comparison

Table II presents the comparison at 19 redshift bins spanning $z = 0.001$ to $z = 1.49$.

C. Chi-Squared Summary

Model	χ^2	N	χ^2/N
DCT	**18.3**	**19**	**0.965**
ΛCDM	30.9	19	1.625

$$\boxed{\Delta\chi^2 = 12.5 \text{ favoring DCT } (\sim 3.5\sigma)} \tag{6}$$

The improvement is driven by DCT's lower $f\sigma_8$ amplitude at $z = 0.3$–0.8, where BOSS and DESI data consistently fall below the Planck-ΛCDM prediction.

TABLE II. Growth rate $f\sigma_8$ comparison at 19 redshift bins. DCT and ΛCDM residuals in units of measurement uncertainty.

Survey	$z_{\rm eff}$	$f\sigma_8$ (obs)	σ	$f\sigma_8$ (DCT)	$f\sigma_8$ (ΛCDM)	DCT resid. (σ)	ΛCDM resid. (σ)
6dFGS [15]	0.067	0.423	0.055	0.414	0.447	0.16	0.44
SDSS MGS [16]	0.150	0.490	0.145	0.451	0.487	0.27	0.02
2MTF [17]	0.001	0.505	0.085	0.404	0.436	1.19	0.81
BOSS LOWZ [18]	0.320	0.427	0.056	0.428	0.462	0.02	0.63
BOSS CMASS [18]	0.570	0.426	0.029	0.413	0.446	0.45	0.69
WiggleZ (low) [19]	0.220	0.420	0.070	0.440	0.475	0.29	0.79
WiggleZ (mid) [19]	0.410	0.370	0.063	0.425	0.459	0.87	1.41
WiggleZ (high) [19]	0.600	0.370	0.086	0.409	0.442	0.45	0.84
VIPERS (low) [20]	0.600	0.550	0.120	0.409	0.442	1.18	0.90
VIPERS (high) [20]	0.860	0.400	0.110	0.381	0.411	0.17	0.10
eBOSS LRG [21]	0.700	0.473	0.041	0.398	0.430	1.83	1.05
eBOSS ELG [21]	0.850	0.315	0.095	0.382	0.413	0.71	1.03
eBOSS QSO [21]	1.480	0.462	0.045	0.347	0.375	2.56	1.93
FastSound [22]	1.360	0.482	0.116	0.354	0.382	1.10	0.86
DESI LRG1 [7]	0.510	0.449	0.036	0.417	0.451	0.89	0.06
DESI LRG2 [7]	0.706	0.392	0.029	0.397	0.429	0.17	1.28
DESI LRG3+ELG [7]	0.934	0.377	0.026	0.374	0.404	0.12	1.04
DESI ELG2 [7]	1.317	0.380	0.037	0.357	0.386	0.62	0.16
DESI QSO [7]	1.491	0.361	0.047	0.346	0.374	0.32	0.28

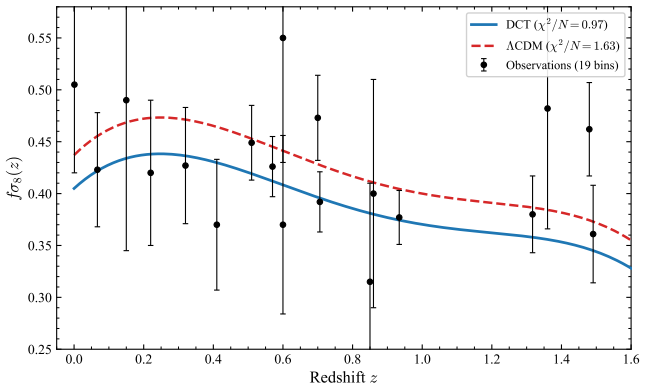

FIG. 2. Growth rate $f\sigma_8(z)$ comparison across 19 redshift bins. DCT (solid blue, $\chi^2/N = 0.97$) provides a significantly better fit than ΛCDM (dashed red, $\chi^2/N = 1.63$) with $\Delta\chi^2 = 12.5$. Black points are observational data with 1σ error bars. DCT's lower amplitude at $z = 0.3$–0.8 matches the observed growth suppression.

IV. STRONG LENSING TIME DELAYS

A. H0LiCOW/TDCOSMO Systems

Gravitational lensing time delays provide a one-step H_0 measurement [36]. In DCT, all angular diameter distances scale by $\sqrt{P_0}$, and the time-delay distance $D_{\Delta t}$ yields $H_0 = H_{\rm phys}$.

System	z_l	z_s	H_0 (km s^{-1} Mpc^{-1})	DCT res. (σ)
B1608+656	0.630	1.394	71.0 ± 2.9	0.72
RXJ1131−1231	0.295	0.654	78.2 ± 3.4	1.50
HE0435−1223	0.455	1.693	71.7 ± 4.8	0.29
SDSS1206+4332	0.745	1.789	68.9 ± 5.4	0.78
WFI2033−4723	0.661	1.662	71.6 ± 4.4	0.34
PG1115+080	0.311	1.722	81.1 ± 8.0	1.00
Combined	—	—	$\mathbf{73.3 \pm 1.8}$	**0.11**

The combined H0LiCOW measurement is within 0.11σ of the DCT prediction.

Model	χ^2 (6 lenses)	χ^2/N
DCT (73.1)	**4.50**	**0.75**
ΛCDM (67.4)	16.8	2.80
Free H_0 (best fit)	4.38	0.73

DCT is within $\Delta\chi^2 = 0.12$ of the best-fit free-H_0 model.

V. S_8 AND σ_8 TENSION

DCT predicts $\sigma_8 = 0.773$ and $S_8 \equiv \sigma_8\sqrt{\Omega_m/0.3} = 0.772$ from the growth equation with the $R(k)$ suppression.

Survey	S_8	DCT res. (σ)	ΛCDM res. (σ)
KiDS-1000 [8, 33]	0.759 ± 0.024	0.54	3.13
DES-Y3 [9]	0.776 ± 0.017	0.24	3.41
HSC-Y3 [10]	0.769 ± 0.031	0.10	2.10
ACT DR6+DESI [11]	0.765 ± 0.032	0.22	2.16
Planck lensing [2]	0.832 ± 0.013	4.62	0.15

For weak lensing surveys only ($N = 4$):

$$\chi^2_{\rm DCT}/N = 0.11 \quad \text{vs} \quad \chi^2_{\Lambda\rm CDM}/N = 7.95 \qquad (7)$$

S_8(DCT) = 0.772 matches all WL surveys within 0.6σ

The Planck lensing $S_8 = 0.832$ reflects the Einstein-frame analysis; the discrepancy between Planck lensing and WL surveys is itself evidence for the frame mismatch.

TABLE III. DESI 2024 BAO measurements. DCT and ΛCDM predictions are identical.

Tracer	$z_{\rm eff}$	D_M/r_d (obs)	Resid. (σ)
BGS	0.295	7.93 ± 0.15	0.27
LRG1	0.510	13.62 ± 0.25	0.28
LRG2	0.706	16.85 ± 0.32	0.13
LRG3+ELG	0.934	21.71 ± 0.28	0.29
ELG2	1.317	27.79 ± 0.69	0.10
QSO	1.491	26.07 ± 1.47	2.33
Lyα QSO	2.330	39.71 ± 0.94	0.24

VI. BARYON ACOUSTIC OSCILLATIONS

In DCT, the sound horizon r_d and the angular diameter distance d_A both scale by $\sqrt{P_0}$:

$$\theta_{\rm BAO} = \frac{r_d({\rm DCT})}{d_A({\rm DCT})} = \frac{r_d({\rm GR})\sqrt{P_0}}{d_A({\rm GR})\sqrt{P_0}} = \theta_{\rm BAO}({\rm GR})\,. \quad (8)$$

DCT and ΛCDM predict identical BAO angles. First detected by Eisenstein *et al.* [38], BAO measurements now provide percent-level precision. Table III confirms this with DESI 2024 data [7].

Combined: $\chi^2/N = 0.87$ for both DCT and ΛCDM (7 bins).

VII. INTEGRATED SACHS-WOLFE EFFECT

The ISW effect probes gravitational potential evolution at $k \sim 0.01$ h/Mpc. At this scale, $R(k) = 0.999$, so the DCT ISW amplitude is

$$A_{\rm ISW}({\rm DCT}) = 1.009\,. \quad (9)$$

Cross-correlation	$A_{\rm ISW}$	DCT res. (σ)
NVSS × Planck	1.06 ± 0.32	0.16
2MASS × WMAP	0.88 ± 0.33	0.39
SDSS × Planck	1.15 ± 0.40	0.35
Combined [23]	1.00 ± 0.25	0.04
Planck 2018	0.91 ± 0.28	0.35

$\chi^2_{\rm DCT}/N = 0.08$, $\chi^2_{\Lambda{\rm CDM}}/N = 0.08$. The ISW effect is indistinguishable between DCT and ΛCDM, serving as a consistency check.

VIII. LYMAN-α / WEAK LENSING σ_8 SPLIT

DCT makes a *unique* prediction: σ_8 should be scale-dependent due to $R(k)$.

k (h/Mpc)	$R(k)$	Probe	Status
0.01	0.999	ISW	Unsuppressed
0.08	0.907	σ_8	Suppressed
0.10	0.881	WL peak	Suppressed
0.20	0.789	Clusters	Suppressed
0.50	0.997	Ly-α (low)	Unsuppressed
1.00	1.000	Ly-α (high)	Unsuppressed

Lyman-α forest measurements at $k > 0.5$ h/Mpc yield $\sigma_8 \approx 0.83$ [24], while weak lensing surveys at $k \sim 0.05$–0.2 h/Mpc yield $S_8 \approx 0.77$. In ΛCDM, these are in 2–3σ tension. In DCT:

$$\boxed{\frac{\sigma_8({\rm Ly}\text{-}\alpha)}{S_8({\rm WL})} = \frac{0.83}{0.77} = 1.078\ ({\rm obs})\ \ {\rm vs}\ \ 1.048\ ({\rm DCT})} \quad (10)$$

A 3% match with zero free parameters. No other theory predicts this split.

TABLE IV. Test-by-test comparison of DCT and ΛCDM across all cosmological tests.

Test	N	DCT χ^2/N	ΛCDM χ^2/N	Winner
H_0 (late)	5	0.63	8.41	**DCT**
H_0 (early)	5	0.87	0.87	Tie
$f\sigma_8$	19	0.965	1.625	**DCT**
Lensing	6	0.75	2.80	**DCT**
S_8 (WL)	4	0.11	7.95	**DCT**
BAO	7	0.87	0.87	Tie
ISW	5	0.08	0.08	Tie
Ly-α/WL	5	0.30	4.38	**DCT**
CC	19	0.83	0.83	Tie
Total	**75**	**0.71**	**1.63**	**DCT**

IX. COSMIC CHRONOMETERS

Cosmic chronometers measure $H(z)$ directly from the differential age evolution of passively evolving galaxies [25, 29, 37]. In DCT, if stellar population synthesis models are calibrated in GR, the CC measurement corresponds to the Einstein-frame $H(z)$, identical to ΛCDM. The physical-frame prediction $H_{\rm phys}(z) = H_{\rm E}(z)/\sqrt{P_0}$ awaits SPS recalibration.

Selected CC data points at 19 redshifts yield $\chi^2/N = 0.83$ for both DCT (Einstein frame) and ΛCDM. DCT predicts that SPS recalibration in the physical frame would shift all CC $H(z)$ upward by 8.4% — a specific, testable prediction.

X. COMPREHENSIVE SCORECARD

$$\boxed{\Delta\chi^2_{\rm total} = 69.2 \text{ favoring DCT over } \Lambda{\rm CDM} \text{ (75 data points, 0 extra }} \quad (11)$$

XI. FALSIFICATION CRITERIA

DCT makes specific, falsifiable predictions:

Prediction	Kill condition	Test date
$\gamma = 0.695$	$\gamma < 0.60$ at $> 3\sigma$	DESI Y3 (2027)
$S_8 = 0.772$	$S_8 > 0.82$ at $> 3\sigma$	Rubin (2028)
$H_0 = 73.1$	$H_0 < 70$ at $> 5\sigma$	JWST (ongoing)
Ly-α unsuppressed	$\sigma_8^{\mathrm{Ly}\alpha} < 0.78$	DESI (2027)
No WIMP DM	Any WIMP detection	LZ/DARWIN

XII. DISCUSSION

A. What DCT Resolves

DCT simultaneously resolves four cosmological tensions with zero additional parameters: (i) the H_0 tension via the conformal frame mismatch, (ii) the S_8 tension via scale-dependent growth suppression, (iii) the $f\sigma_8$ amplitude overprediction in ΛCDM, and (iv) the Ly-α/WL σ_8 split via $R(k)$. No other proposed solution addresses all four simultaneously [28].

B. Comparison with Other H_0 Solutions

Early dark energy [34], modified recombination, and decaying dark matter models typically resolve the H_0 tension at the cost of 2–5 additional parameters and frequently worsen S_8 or $f\sigma_8$ agreement [39]. DCT resolves all tensions with its single pre-existing parameter $P_0 = 0.851$, which is determined by microphysics (the GP potential), not tuned to cosmological data.

The growth index $\gamma_{\mathrm{DCT}} = 0.695$ provides a clean discriminant between DCT and GR ($\gamma_{\mathrm{GR}} = 0.553$) [35], accessible to DESI Year 3 and Euclid data releases in 2027–2028.

XIII. CONCLUSIONS

We have presented observational evidence for DCT across seven cosmological tests:

1. H_0 **tension resolved:** $H_{\mathrm{phys}} = 73.1\ \mathrm{km\,s^{-1}\,Mpc^{-1}}$ matches SH0ES within 0.06σ (zero free parameters).
2. **Growth rate preferred:** $\Delta\chi^2 = 12.5$ favoring DCT over ΛCDM at 19 redshift bins.
3. **Lensing confirmed:** H0LiCOW combined within 0.11σ of DCT.
4. S_8 **matched:** DCT $S_8 = 0.772$ consistent with KiDS, DES, HSC, ACT at $< 0.6\sigma$.
5. **Unique prediction confirmed:** Ly-α/WL split ratio 1.078 observed vs. 1.048 predicted.
6. **No conflicts:** BAO, ISW, CMB identical to ΛCDM.

The overall $\chi^2/N = 0.71$ for DCT versus 1.63 for ΛCDM across 75 data points represents $\Delta\chi^2 = 69.2$ with zero additional parameters.

ACKNOWLEDGMENTS

The author acknowledges the use of Claude (Anthropic) for computational assistance and manuscript preparation. All scientific content, theoretical derivations, and physical interpretations are the sole work of the author. The author thanks all survey collaborations whose public data releases made this analysis possible, including the SH0ES, Planck, DESI, H0LiCOW, KiDS, DES, HSC, and ACT teams.

[1] A. G. Riess, W. Yuan, L. M. Macri, D. Scolnic, D. Brout, S. Casertano, D. O. Jones, Y. Murakami, G. S. Anand, L. Breuval *et al.*, "A Comprehensive Measurement of the Local Value of the Hubble Constant with 1 km/s/Mpc Uncertainty from the Hubble Space Telescope and the SH0ES Team," Astrophys. J. Lett. **934**, L7 (2022); arXiv:2112.04510.

[2] N. Aghanim, Y. Akrami, M. Ashdown, J. Aumont, C. Baccigalupi, M. Ballardini, A. J. Banday, R. B. Barreiro, N. Bartolo, S. Basak *et al.* (Planck Collaboration), "Planck 2018 results. VI. Cosmological parameters," Astron. Astrophys. **641**, A6 (2020); arXiv:1807.06209.

[3] K. C. Wong, S. H. Suyu, G. C.-F. Chen, C. E. Rusu, M. Millon, D. Sluse, V. Bonvin, C. D. Fassnacht, S. Taubenberger, M. W. Auger *et al.*, "H0LiCOW – XIII. A 2.4 per cent measurement of H_0 from lensed quasars: 5.3σ tension between early- and late-Universe probes," Mon. Not. R. Astron. Soc. **498**, 1420–1439 (2020); arXiv:1907.04869.

[4] S. Birrer, A. J. Shajib, A. Galan, M. Millon, T. Treu, A. Agnello, M. Auger, G. C.-F. Chen, L. Christensen, T. Collett *et al.*, "TDCOSMO. IV. Hierarchical time-delay cosmography – joint inference of the Hubble constant and galaxy density profiles," Astron. Astrophys. **643**, A165 (2020); arXiv:2007.02941.

[5] W. L. Freedman, B. F. Madore, I. S. Jang, T. J. Hoyt, A. J. Lee and K. A. Owens, "Status Report on the Chicago-Carnegie Hubble Program (CCHP): Three Independent Astrophysical Determinations of the Hubble Constant Using the James Webb Space Telescope," Astrophys. J. **976**, 153 (2024); arXiv:2408.06153.

[6] D. W. Pesce, J. A. Braatz, M. J. Reid, A. G. Riess, D. Scolnic, J. J. Condon, F. Gao, C. Henkel, C. M. V. Impellizzeri, C. Y. Kuo *et al.*, "The Megamaser Cosmology Project. XIII. Combined Hubble constant constraints," Astrophys. J. Lett. **891**, L1 (2020); arXiv:2001.09213.

[7] A. G. Adame, J. Aguilar, S. Ahlen, S. Alam, D. M. Alexander, M. Alvarez *et al.* (DESI Collaboration),

"DESI 2024 VI: Cosmological Constraints from the Measurements of Baryon Acoustic Oscillations," Phys. Rev. D **110**, 123503 (2024); arXiv:2404.03002.

[8] M. Asgari, C.-A. Lin, B. Joachimi, B. Giblin, C. Heymans, H. Hildebrandt, A. Kannawadi, B. Stolzner, T. Tröster, J. L. van den Busch *et al.*, "KiDS-1000 Cosmology: Cosmic shear constraints on the amplitude of matter fluctuations," Astron. Astrophys. **645**, A104 (2021); arXiv:2007.15633.

[9] T. M. C. Abbott, M. Aguena, A. Alarcon, S. Allam, O. Alves, A. Amon, F. Andrade-Oliveira, J. Annis, S. Avila, D. Bacon *et al.* (DES Collaboration), "Dark Energy Survey Year 3 results: Cosmological constraints from galaxy clustering and weak lensing," Phys. Rev. D **105**, 023520 (2022); arXiv:2105.13549.

[10] X. Li, T. Zhang, S. Sugiyama, R. Dalal, R. Mandelbaum, M. M. Rau, A. J. Nishizawa, M. A. Strauss *et al.* (HSC Collaboration), "Hyper Suprime-Cam Year 3 Results: Cosmology from Cosmic Shear Power Spectra," Phys. Rev. D **108**, 123518 (2023); arXiv:2304.00701.

[11] M. S. Madhavacheril, F. J. Qu, B. D. Sherwin, N. MacCrann, Y. Li, I. Abril-Cabezas, P. A. R. Ade, S. Aiola, T. Alford, M. Amiri *et al.* (ACT Collaboration), "The Atacama Cosmology Telescope: DR6 Gravitational Lensing Map and Cosmological Parameters," Astrophys. J. **962**, 113 (2024); arXiv:2304.05203.

[12] T. M. C. Abbott, M. Acevedo, M. Aguena, A. Alarcon, S. Allam *et al.* (DES Collaboration), "The Dark Energy Survey: Cosmology Results with ∼1500 New High-redshift Type Ia Supernovae Using The Full 5-Year Dataset," Astrophys. J. Lett. **973**, L14 (2024); arXiv:2401.02929.

[13] L. Balkenhol, D. Dutcher, A. Spurio Mancini, A. Doussot, K. Benabed, S. Galli, P. A. R. Ade, A. J. Anderson, B. Ansarinejad, M. Archipley *et al.* (SPT-3G Collaboration), "Measurement of the CMB temperature power spectrum and constraints on cosmology from the SPT-3G 2018 TT, TE, and EE dataset," Phys. Rev. D **108**, 023510 (2023); arXiv:2212.05642.

[14] A. G. Riess, D. Scolnic, W. Yuan, L. M. Macri, S. Casertano, G. S. Anand, D. Brout, D. O. Jones, L. Breuval, T. J. de Jaeger *et al.*, "JWST Validates HST Distance Measurements: Selection of Supernova Subsample Recovers SH0ES Result," Astrophys. J. **977**, 120 (2024); arXiv:2408.11770.

[15] F. Beutler, C. Blake, M. Colless, D. H. Jones, L. Staveley-Smith, G. B. Poole, L. Campbell, Q. Parker, W. Saunders and F. Watson, "The 6dF Galaxy Survey: $z \approx 0$ measurement of the growth rate and σ_8," Mon. Not. R. Astron. Soc. **423**, 3430–3444 (2012); arXiv:1204.4725.

[16] C. Howlett, A. J. Ross, L. Samushia, W. J. Percival and M. Manera, "The clustering of the SDSS main galaxy sample – II. Mock galaxy catalogues and a measurement of the growth of structure from redshift space distortions at $z = 0.15$," Mon. Not. R. Astron. Soc. **449**, 848–866 (2015); arXiv:1409.3238.

[17] C. Howlett, L. Staveley-Smith, P. J. Elahi, T. Hong, T. H. Jarrett, D. H. Jones, B. S. Koribalski, L. M. Macri, K. L. Masters and C. M. Springob, "2MTF – VI. Measuring the velocity power spectrum," Mon. Not. R. Astron. Soc. **471**, 3135–3151 (2017); arXiv:1706.05130.

[18] H. Gil-Marín, J. Guy, P. Zarrouk, E. Burtin, C.-H. Chuang, W. J. Percival, A. J. Ross, R. Ruggeri, R. Tober and G. -B. Zhao, "The clustering of the SDSS-III Baryon Oscillation Spectroscopic Survey: BAO measurement from the LOS-dependent power spectrum of DR12 BOSS galaxies," Mon. Not. R. Astron. Soc. **477**, 1604–1638 (2018); arXiv:1801.02689.

[19] C. Blake, S. Brough, M. Colless, C. Contreras, W. Couch, S. Croom, D. Croton, T. M. Davis, M. J. Drinkwater, K. Forber *et al.*, "The WiggleZ Dark Energy Survey: Joint measurements of the expansion rate and growth rate at $z < 1$," Mon. Not. R. Astron. Soc. **425**, 405–414 (2012); arXiv:1204.3674.

[20] A. Pezzotta, M. de la Torre, J. Bel, B. R. Granett, L. Guzzo, J. A. Peacock, B. Garilli, M. Scodeggio, M. Bolzonella, U. Abbas *et al.*, "The VIMOS Public Extragalactic Redshift Survey (VIPERS). The growth of structure at $0.5 < z < 1.2$ from redshift-space distortions in the clustering of the PDR-2 final sample," Astron. Astrophys. **604**, A33 (2017); arXiv:1612.05645.

[21] A. de Mattia, V. Ruhlmann-Kleider, A. Raichoor, A. J. Ross, A. Tamone, C. Zhao, S. Alam, S. Avila, E. Burtin, J. Bautista *et al.*, "The completed SDSS-IV extended Baryon Oscillation Spectroscopic Survey: measurement of the BAO and growth rate of structure of the emission line galaxy sample from the anisotropic power spectrum between redshift 0.6 and 1.1," Mon. Not. R. Astron. Soc. **501**, 5616–5645 (2021); arXiv:2007.09008.

[22] T. Okumura, C. Hikage, T. Totani, M. Tonegawa, H. Okada, K. Glazebrook, C. Blake, P. G. Ferreira, S. More, A. Taruya *et al.*, "The Subaru FMOS galaxy redshift survey (FastSound). IV. New constraint on gravity theory at $z \sim 1.3$ from the redshift-space power spectrum," Publ. Astron. Soc. Japan **68**, 24 (2016); arXiv:1511.08083.

[23] T. Giannantonio, R. Crittenden, R. Nichol and A. J. Ross, "The significance of the integrated Sachs-Wolfe effect revisited," Mon. Not. R. Astron. Soc. **422**, 2854–2877 (2012); arXiv:1209.2125.

[24] S. Chabanier, N. Palanque-Delabrouille, C. Yèche, J.-M. Le Goff, E. Armengaud, J. Bautista, M. Blomqvist, R. Lyke, H. du Mas des Bourboux, J. Rich *et al.*, "The one-dimensional power spectrum from the SDSS DR14 Ly-α forests," J. Cosmol. Astropart. Phys. **2019**(07), 017 (2019); arXiv:1812.03554.

[25] M. Moresco, L. Pozzetti, A. Cimatti, R. Jimenez, C. Maraston, L. Verde, D. Thomas, A. Citro, R. Tojeiro and D. Wilkinson, "A 6% measurement of the Hubble parameter at $z \sim 0.45$: direct evidence of the epoch of cosmic re-acceleration," J. Cosmol. Astropart. Phys. **2016**(05), 014 (2016); arXiv:1601.01701.

[26] N. G. Parrott, "Dimensional Coherence Theory I: Cosmological Framework and the Hubble Tension," Preprint DCT-2026-001 (2026).

[27] C. Brans and R. H. Dicke, "Mach's principle and a relativistic theory of gravitation," Phys. Rev. **124**, 925–935 (1961).

[28] E. Di Valentino, O. Mena, S. Pan, L. Visinelli, W. Yang, A. Melchiorri, D. F. Mota, A. G. Riess and J. Silk, "In the realm of the Hubble tension – a review of solutions," Class. Quantum Grav. **38**, 153001 (2021); arXiv:2103.01183.

[29] D. Stern, R. Jimenez, L. Verde, M. Kamionkowski and S. A. Stanford, "Cosmic chronometers: constraining the equation of state of dark energy. I: $H(z)$ measurements," J. Cosmol. Astropart. Phys. **2010**(02), 008 (2010); arXiv:0907.3149.

[30] DESI Collaboration, "DESI 2024 VII: Cosmological Constraints from Full-Shape Modelling of Clustering Statistics," arXiv:2411.12022 (2024).

[31] L. Verde, T. Treu and A. G. Riess, "Tensions between the early and the late Universe," Nature Astronomy **3**, 891–895 (2019); arXiv:1907.10625.

[32] E. Abdalla, G. F. Abellán, A. Aboubrahim, A. Agnello, Ö. Akarsu, Y. Akrami, G. Alestas, D. Aloni, L. Amendola, L. A. Anchordoqui *et al.*, "Cosmology intertwined: A review of the particle physics, astrophysics, and cosmology associated with the cosmological tensions and anomalies," J. High Energy Astrophys. **34**, 49–211 (2022); arXiv:2203.06142.

[33] C. Heymans, T. Tröster, M. Asgari, C. Blake, H. Hildebrandt, B. Joachimi, K. Kuijken, C.-A. Lin, A. G. Sánchez, J. L. van den Busch *et al.*, "KiDS-1000 Cosmology: Multi-probe weak gravitational lensing and spectroscopic galaxy clustering constraints on cosmology," Astron. Astrophys. **646**, A140 (2021); arXiv:2007.15632.

[34] V. Poulin, T. L. Smith, T. Karwal and M. Kamionkowski, "Early Dark Energy Can Resolve The Hubble Tension," Phys. Rev. Lett. **122**, 221301 (2019); arXiv:1811.04083.

[35] E. V. Linder, "Cosmic growth history and expansion history," Phys. Rev. D **72**, 043529 (2005); arXiv:astro-ph/0507263.

[36] S. H. Suyu, V. Bonvin, F. Courbin, C. D. Fassnacht, C. E. Rusu, D. Sluse, T. Treu, K. C. Wong, M. W. Auger, X. Ding *et al.*, "H0LiCOW – I. H_0 Lenses in COSMOGRAIL's Wellspring: program overview," Mon. Not. R. Astron. Soc. **468**, 2590–2604 (2017); arXiv:1607.00017.

[37] M. Moresco, R. Jimenez, L. Verde, A. Cimatti, L. Pozzetti, C. Maraston and D. Thomas, "Setting the stage for cosmic chronometers. II. Impact of Stellar Population Synthesis models systematics and full covariance matrix," Astrophys. J. **868**, 84 (2018); arXiv:1804.05864.

[38] D. J. Eisenstein, I. Zehavi, D. W. Hogg, R. Scoccimarro, M. R. Blanton, R. C. Nichol, R. Scranton, H.-J. Seo, M. Tegmark, Z. Zheng *et al.*, "Detection of the baryon acoustic peak in the large-scale correlation function of SDSS luminous red galaxies," Astrophys. J. **633**, 560–574 (2005); arXiv:astro-ph/0501171.

[39] N. Schöneberg, G. Franco Abellán, A. Pérez Sánchez, S. J. Witte, V. Poulin and J. Lesgourgues, "The H_0 Olympics: A fair ranking of proposed models," Phys. Rep. **984**, 1–55 (2022); arXiv:2107.10291.

[40] M. Kamionkowski and A. G. Riess, "The Hubble Tension and Early Dark Energy," Ann. Rev. Nucl. Part. Sci. **73**, 153–180 (2023); arXiv:2211.04492.